Modeling survival probabilities of superheavy nuclei at high excitation energies

C. Y. Qiao and J. C. Pei*

State Key Laboratory of Nuclear Physics and Technology, School of Physics, Peking University, Beijing 100871, China

(Received 5 May 2022; revised 13 June 2022; accepted 30 June 2022; published 15 July 2022)

This work investigated the first-chance survival probabilities of highly excited compound superheavy nuclei in the prospect of synthesizing new superheavy elements. The main feature of our modelings is the adoption of microscopic temperature dependent fission barriers in calculations of fission rates. A simple derivation is demonstrated to elucidate the connection between the Bohr-Wheeler statistical model and the imaginary free energy method, obtaining a new formula for fission rates. Various models are examined to reproduce the experimental fission probability of ^{210}Po. Systematic studies of fission and survival probabilities of No, Fl, Og, and $Z = 120$ compound nuclei are performed. Results show that $Z = 120$ compound nuclei still have considerable first-chance survival probabilities at high excitations, which are very similar to that of Fl and Og nuclei.

DOI: 10.1103/PhysRevC.106.014608

I. INTRODUCTION

To synthesize the heaviest elements is one of the major science problems [1,2]. To date, superheavy elements $Z =$ 107–113 [3–9] have been synthesized in cold fusion reactions with the target Pb or Bi, and $Z =$ 114–118 [10–14] have been synthesized in hot fusion reactions with the projectile ^{48}Ca. The seventh row of the periodic table of elements has been completed. In order to produce superheavy elements in the eighth row, experimental attempts to synthesize $Z = 119$ and 120 were performed in laboratories using reactions such as ^{58}Fe + ^{244}Pu [15] at JINR, ^{51}V + ^{248}Cm [16] at RIKEN, and ^{64}Ni + ^{238}U, ^{50}Ti + ^{249}Bk, ^{50}Ti + ^{249}Cf, ^{54}Cr + ^{248}Cm [17–19] at GSI, but no evidence of new elements was observed. Currently, the measured sensitivity of cross sections has reached 65 fb for searching the next superheavy element [18]. The main issue is to design the optimal combination of beam-target nuclei and the bombarding energy. In this context, reliable theoretical guidance would be valuable for such extremely difficult experiments.

Theoretically, the synthesis process of superheavy nuclei can be described as the capture-fusion-evaporation reaction. In this procedure the residue cross section is written as [20]

$$\sigma_{ER} = \sigma_{\rm cap} P_{\rm CN} W_{\rm sur}, \tag{1}$$

which depends on the capture cross-section $\sigma_{\rm cap}$, the fusion probability $P_{\rm CN}$ to compound nuclei, and the survival probability $W_{\rm sur}$ of excited compound nuclei. The survival probabilities of compound nuclei are determined by the competition between the neutron emission rates and fission rates. There are many models that have been developed to predict the synthesis of superheavy nuclei [21–26]. The combined modelings of three steps can result in large uncertainties. In particular, the surprisingly large cross sections of hot fusion reactions indicate that microscopic calculations of survival probabilities are essential [27–29]. Thus reliable modelings of survival probabilities are important since such experimental constraints in the superheavy region are rare.

Conventionally, the statistical models have been widely used for calculations of survival probabilities of compound nuclei [30–32]. The statistical models can be traced back to Weisskopf's work for particle evaporations in 1937 [33] and Bohr-Wheeler's work for fission rates in 1939 [34]. The Bohr-Wheeler statistical model is based on the classical transition state theory, which relies on fission barriers and level densities. Actually, the fission barriers and level density parameters could be dependent on temperatures (or excitation energies), nuclear deformations, and shell structures. Consequently, statistical models have to adopt parametrized energy dependent corrections to fission barriers and level density parameters [35]. In the standard statistical model, the fission barrier is energy independent. However, energy dependent fission barriers are necessary to obtain reasonable fission observables such as survival probabilities [36] and fission product yields [37].

The thermal fission rates can also be calculated by the dynamical Kramers model [38] and the imaginary free energy approach (ImF) [39]. ImF can, in principle, describe the fission rates from low to high excitation energies in the quantum statistical framework. The fission barrier heights and the curvatures around the equilibrium point and the saddle point are essential inputs for the Kramers and ImF methods [40]. This can also be microscopically estimated but has rarely been discussed. Strutinsky pointed out a systematic difference between the Karmers model and the Bohr-Wheeler model [41,42]. It is interesting to elucidate the connections between the Bohr-Wheeler, Kramers, and ImF models.

In this work, our main goal is to study the survival probabilities of superheavy compound nuclei in the microscopic framework based on the finite-temperature Skyrme-Hartree-

*peij@pku.edu.cn

Fock+BCS approach [43]. The fission barriers are given in terms of free energies and are energy dependent. Then the fission rates are obtained with ImF [39,40], the Bohr-Wheeler model [34], and the Kramers model [38]. The neutron evaporation rates can be obtained by the standard statistical model. For comparison, neutron evaporation rates are also estimated by the density of neutron gases around nuclear surfaces [44]. The connections among three fission models are discussed. To benchmark different models, the fission probabilities of ^{210}Po up to high excitations are studied before being extrapolated to the superheavy region.

II. THEORETICAL FRAMEWORK

A. Finite-temperature Hartree-Fock+BCS calculations

In this work, the fission barriers are calculated with Skyrme-Hartree-Fock+BCS at finite temperatures (FT-BCS) [43]. Previously we have studied the fission barriers with the finite-temperature Hartree-Fock-Bogoliubov method [28,45], which is computationally more expensive. For systematic calculations, FT-BCS calculations are performed with the SkyAX solver in cylindrical coordinate spaces [46]. The Skyrme interaction SkM* [47] and the mixed pairing interaction [48] are used. Note that SkM* was developed particularly for descriptions of fission barriers.

In FT-BCS, the normal density ρ and the pairing density $\tilde{\rho}$ at a finite temperature are modified as [43]

$$\rho_T(r) = \sum_i \left[u_i^2 f_i + \upsilon_i^2(1-f_i)\right]|\phi_i(r)|^{2,} \tag{2}$$

$$\tilde{\rho}_T(r) = \sum_i u_i \upsilon_i (1-2f_i)|\phi_i(r)|^{2,} \tag{3}$$

where $f_i = 1/(1+\mathrm{e}^{E_i/kT})$ (kT is the temperature in MeV) is the temperature dependent factor; E_i is the quasiparticle energy; k is the Boltzmann constant. The entropy S is evaluated as

$$S = -k\sum_i [f_i \ln f_i + (1-f_i)\ln(1-f_i)]. \tag{4}$$

The temperature dependent fission barriers are calculated in terms of the free energy $F = E_T - TS$, where E_T is the intrinsic binding energy based on the temperature-dependent densities.

For realistic calculations, we also need mass parameters which are obtained by the Cranking formula [49]. At a finite temperature, the resulting mass parameters have significant fluctuations as a function of deformations [40]. However, the mass parameters extracted from microscopic dynamical calculations are not much dependent on excitation energies [50,51]. Therefore we adopt the mass parameters at zero temperature in all calculations.

It has been demonstrated that uniform neutron-gas density distributions can be obtained in coordinate-space FT-HFB calculations [28,44]. This also appears in coordinate-space FT-BCS calculations. With the uniform neutron gas density n_{gas}, the neutron emission width Γ_n is given by the nucleosynthesis formula [52]

$$\Gamma_n = \hbar n_{\mathrm{gas}} \langle \sigma \upsilon \rangle, \tag{5}$$

where σ is the neutron capture cross section and estimated by the geometric area πR^2. $\langle \upsilon \rangle$ is the average velocity of the external gas. This method does not involve level densities, see details in Ref. [44].

B. Imaginary free energy method

The imaginary free energy method (ImF) can, in principle, describe a system's metastability from quantum tunneling at low temperatures to statistical decays at high temperatures in a consistent framework [39]. In ImF, the fission barrier is naturally given by temperature dependent free energies. This method has been previously used to evaluate fission rates of compound nuclei [40]. At low temperatures, the ImF formula for the fission width from excited systems is given as [39]

$$\begin{aligned} \Gamma_f &= \frac{1}{Z_0}\frac{1}{2\pi\hbar}\int_0^{V_b} P(E)\exp(-\beta E)\,dE, \\ Z_0 &= \left[2\sinh\left(\frac{1}{2}\beta\hbar\omega_0\right)\right]^{-1}, \end{aligned} \tag{6}$$

where ω_0 is the curvature or frequency around the equilibrium point at the potential valley; V_b is the barrier height; Z_0 is the partition function; β denotes $1/kT$; $P(E)$ is the barrier transmission probability.

For the fission probability at high temperatures, the contribution is dominated by reflections above the barriers. In this case, the transmission probability $P(E)$ can be estimated by

$$P(E) = \{1 + \exp[2\pi(E - V_b)/\hbar\omega_b]\}^{-1}. \tag{7}$$

Then the fission width at high temperatures can be written as [39]

$$\Gamma_f = \frac{\omega_b}{2\pi}\frac{\sinh(\frac{1}{2}\beta\hbar\omega_0)}{\sin(\frac{1}{2}\beta\hbar\omega_b)}\exp(-\beta V_b), \tag{8}$$

where ω_b is the curvature at the saddle point of the barrier. The curvatures ω_0 and ω_b can be calculated with the microscopic temperature dependent fission barriers and the mass parameters, as discussed in Ref. [40]. There is a narrow transition in ImF formulas from low to high temperatures, which is dependent on the critical temperature $\hbar\omega_b/2\pi$ [39]. The ImF method has been widely applied in chemical reactions in a thermal bath. In nuclear fission studies, ImF shows that the fission lifetime decreases very rapidly at low excitations and decreases slowly at high excitations [40]. With temperature dependent fission barriers, it is a success for ImF to reveal that the compound nucleus ^{278}Cn in the cold fusion can not survive at high excitations while ^{292}Fl in the hot fusion still has a considerable survival probability at high excitations [40].

C. Bohr-Wheeler statistical model

The Bohr-Wheeler statistical model has widely been used to calculate the survival probabilities of superheavy nuclei [30,31]. This is also known as the transition state theory and is based on the microcanonical ensemble. The width of neutron evaporation is given by [33]

$$\Gamma_n(E) = \frac{2mR^2}{\pi\hbar^2\rho_0(E)}\int_0^{E-S_n} \varepsilon_n \rho_0(E - S_n - \varepsilon_n)\,d\varepsilon_n. \tag{9}$$

Here, m is the neutron mass, R is the radius of the compound nucleus, S_n is the neutron separation energy, and $\rho_0(E)$ is the level density at the equilibrium deformation.

The fission width can be calculated with the Bohr-Wheeler formula as [34]

$$\Gamma_f(E) = \frac{1}{2\pi\rho_0(E)} \int_0^{E-V_b} \rho_s(E - V_b - \varepsilon_f) T_f(\varepsilon_f)\, d\varepsilon_f, \tag{10}$$

where $\rho_s(E)$ is the level density at the saddle point, and $T_f(\varepsilon_f)$ is the barrier transmission probability,

$$T_f(\varepsilon_f) = \left\{1 + \exp\left[-\frac{2\pi\varepsilon_f}{\hbar\omega_{sd}}\right]\right\}^{-1}. \tag{11}$$

Usually $\hbar\omega_{sd}$ is taken as 2.2 MeV in empirical calculations as mentioned in Ref. [32].

The level density is calculated with the Fermi-gas model as [53]

$$\rho(E) = \frac{\sqrt{\pi}\exp(2\sqrt{aE})}{12a^{1/4}E^{5/4}}, \tag{12}$$

where a is the level density parameter taken as the usual $a = A/12$ MeV, the level density parameter at the saddle point is taken as $a_{sd} = 1.1a$. Note that there are modified formulas of energy dependent level densities [35], and associated parameters are dependent on the nuclear region.

D. Connection between Bohr-Wheeler model and ImF

It is interesting to study the connections between the Bohr-Wheeler model and the ImF method for fission rates and survival probabilities of compound nuclei. By Combining Eqs. (6) and (7), the fission width is given as

$$\Gamma_f^{ImF} = Z_0^{-1} \int \frac{1}{2\pi\hbar} \frac{1}{1 + \exp\left(-\frac{2\pi(E-V_b)}{\hbar\omega_b}\right)} \exp(-\beta E)\, dE,$$
$$Z_0 = \left[2\sinh\left(\frac{1}{2}\beta\hbar\omega_0\right)\right]^{-1}, \tag{13}$$

where V_b is the fission barrier height. If we use $\sinh(x) = \frac{e^x - e^{-x}}{2}$ and define $x = E - V_b$, then Eq. (13) can be written as

$$\Gamma_f^{ImF} = \frac{\omega_0\hbar}{2\pi\hbar T} \int \frac{1}{1 + \exp\left(-\frac{2\pi x}{\hbar\omega_b}\right)} \exp\left(-\frac{x}{T}\right) \times \exp\left(-\frac{V_b}{T}\right) dx. \tag{14}$$

For the level density in statistical models, $\ln\rho(E)$ is a smooth curve in terms of E. When ΔE is small, we have

$$\ln\rho(E + \Delta E) = \ln\rho(E) + \left[\frac{d\ln\rho(E)}{dE}\right]\Delta E. \tag{15}$$

Since $\frac{1}{T} = [\frac{d\ln\rho(E)}{dE}]$ is defined by the evaporation model, so we have

$$\rho(E + \Delta E) = \rho(E)\exp\left(\frac{\Delta E}{T}\right), \tag{16}$$

where T is the nuclear temperature. By combining Eqs. (10), (11), and (16), we can get

$$\Gamma_f^{BW} = \frac{1}{2\pi\rho_0(E)} \int_0^{E-V_b} \frac{\rho_s(E - V_b)}{1 + \exp\left(-\frac{2\pi k}{\hbar\omega_b}\right)} \exp\left(-\frac{k}{T}\right) dk. \tag{17}$$

By comparing Eqs. (14) and (17), the connection between the Bohr-Wheeler model and the ImF method is

$$\Gamma_f^{BW} = \frac{T}{\omega_0} \frac{\rho_s(E - V_b)}{\rho_0(E)} \exp\left(\frac{V_b}{T}\right) \Gamma_f^{ImF}. \tag{18}$$

Since the two modelings have different advantages and disadvantages, we now obtain a new formula to calculate the fission width:

$$\Gamma_{f1} = \frac{\rho_s(E - V_b)}{\rho_0(E)} \frac{\omega_b T}{2\pi\omega_0} \frac{\sinh(\frac{1}{2}\beta\hbar\omega_0)}{\sin(\frac{1}{2}\beta\hbar\omega_b)}. \tag{19}$$

This formula is close to the Bohr-Wheeler model. In this case, the formula includes the temperature dependent fission barrier heights in ρ_s and also the influence of the microcanonical statistics. This formula avoids doing integral in statistical calculations of fission rates. It has been pointed out that there is a difference between the Bohr-Wheeler fission model and the Kramers model by a factor ω_0/T [42], then we have another new formula for fission rates:

$$\Gamma_{f2} = \frac{\omega_0}{T}\Gamma_f^{BW} = \frac{\rho_s(E - V_b)}{\rho_0(E)} \frac{\omega_b}{2\pi} \frac{\sinh(\frac{1}{2}\beta\hbar\omega_0)}{\sin(\frac{1}{2}\beta\hbar\omega_b)}. \tag{20}$$

This formula includes ω_0/T, being consistent with ImF and the Kramers model at high temperatures [38]. At very high excitations, the barrier height V_b is small compared to the excitation energy E. By using the relation in Eqs. (16) and (12), then Eq. (18) becomes

$$\Gamma_f^{BW} = \frac{T}{\omega_0} \frac{\exp[2\sqrt{E}(\sqrt{a_{sd}} - \sqrt{a})]}{(a_{sd}/a)^{1/4}} \Gamma_f^{ImF}. \tag{21}$$

If we assume the level density parameters $a_{sd} = a$ at the limit of extremely high excitations, which means quantum shell effects are completely lost, then we have

$$\Gamma_f^{BW} = \frac{T}{\omega_0}\Gamma_f^{ImF}. \tag{22}$$

It demonstrates that results of the Bohr-Wheeler model of the microcanonical ensemble are close to those of ImF in a heat bath at extremely high temperatures, except for the prefactor T/ω_0. Note that ImF is also close to the Kramers model at high temperatures [39].

III. RESULTS AND DISCUSSIONS

First, we calculate the fission probabilities of ^{210}Po to benchmark various models. ^{210}Po has accurate experimental energy dependent fission probabilities [54]. Figure 1 shows the calculated fission widths with different modelings. In these calculations, the energy dependent fission barriers are adopted, which are taken from microscopic finite-temperature

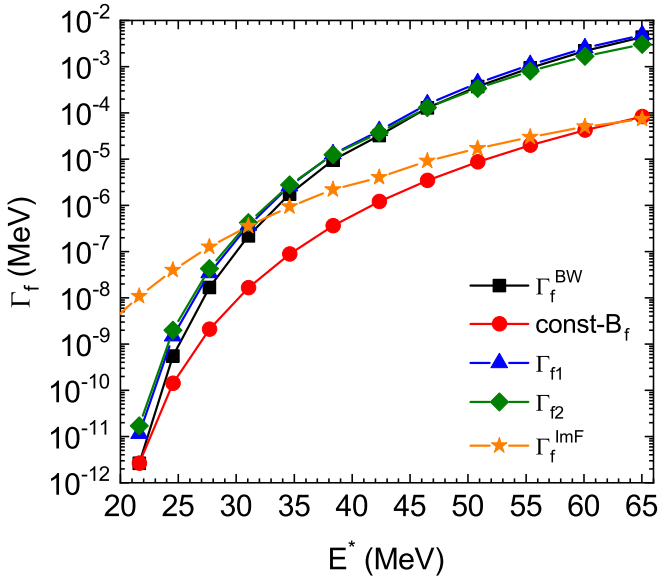

FIG. 1. Calculated fission widths Γ_f of ^{210}Po as a function of excitation energies E^* with different models. The energy dependent fission barriers are used except for const-B_f within the Bohr-Wheeler model. Γ_f^{BW}, Γ_{f1}, Γ_{f2}, Γ_f^{ImF} are obtained with Eqs. (10), (19), (20), (6), respectively.

Hartree-Fock+BCS calculations. We can see that the fission widths calculated with the Bohr-Wheeler model, the formula Γ_{f1} [Eq. (19)], and the formula Γ_{f2} [Eq. (20)] are close. This verified the correctness of Eqs. (19) and (20). In this case, the role of the factor ω_0/T is not significant. The results calculated by ImF are also shown, which are very different from the Bohr-Wheeler results. For example, the ratio difference estimated by Eq. (21) is 26.3 at 65 MeV if we assume $a_{sd} = 1.1a$. This explained that the significant differences between the Bohr-Wheeler model and ImF are due to the different level density parameters between the saddle point and the equilibrium point. Note that in the original Bohr-Wheeler model, the fission barrier is energy independent. We also did calculations with a constant fission barrier height of 19.59 MeV with the Bohr-Wheeler model. We can see that the fission widths with constant fission barriers are much smaller at high excitations. The large discrepancy in fission widths, by using energy-dependent and energy-independent fission barriers, has also been shown in Ref. [55]. This demonstrated the essential role of energy dependent fission barriers in calculations of fission rates.

To compare with the experimental fission probabilities $\Gamma_f/\Gamma_{\rm tot}$ of ^{210}Po, the neutron evaporation widths have to be calculated. The neutron evaporation widths can be calculated by the standard statistical model [Eq. (9)] or by the microscopic neutron gas model [Eq. (5)]. In both calculations, the same nuclear radius R is used for the neutron-reaction cross section πR^2. The calculated fission probabilities are shown in Fig. 2. The experimental $\Gamma_f/\Gamma_{\rm tot}$ of ^{210}Po are taken from proton and α induced fission reactions [54]. It can be seen that all the calculations can reproduce the experimental data. Figure 2(a) shows that the neutron gas model leads to a slightly larger fission probability or a smaller survival probability at

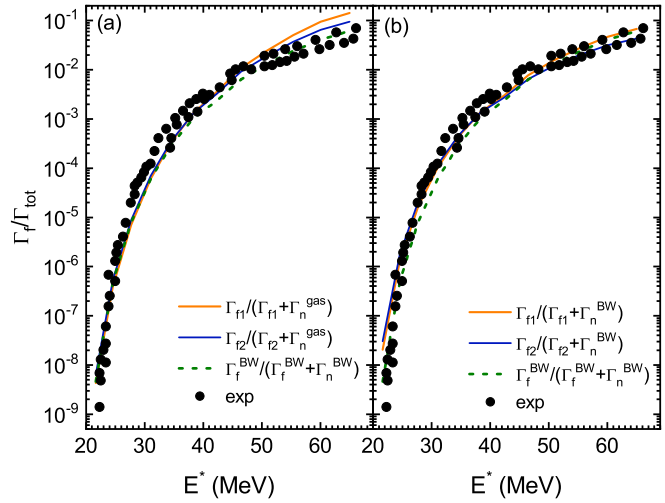

FIG. 2. The results of $\Gamma_f/\Gamma_{\rm tot}$ as a function of E^* for ^{210}Po. Experimental data are taken from Ref. [54]. Different fission widths and neutron emission widths are adopted. See text for details.

high excitations. The factor ω_0/T included in Γ_{f2} results in slightly reduced fission probabilities at high excitations. Other calculations with ImF or constant fission barriers cannot reproduce the experimental data and are not shown.

Next we study the fission and survival probabilities of superheavy compound nuclei with the modelings that can reproduce the fission probabilities of ^{210}Po. In this work, four elements No, Fl, Og, and $Z = 120$ are selected for study. The fission barrier heights as a function of excitation energy E^* are shown in Fig. 3. We see that $Z = 120$ isotopes have considerable fission barriers even at high excitations. For $^{298-304}$120 isotopes, the barrier heights are not sensitive to the neutron numbers. On the other hand, the barrier heights are much more dependent on neutron numbers for $^{288-294}$Fl isotopes. For Fl and Og isotopes, more neutrons result in enhanced fission barriers. Note that the microscopic energy dependence

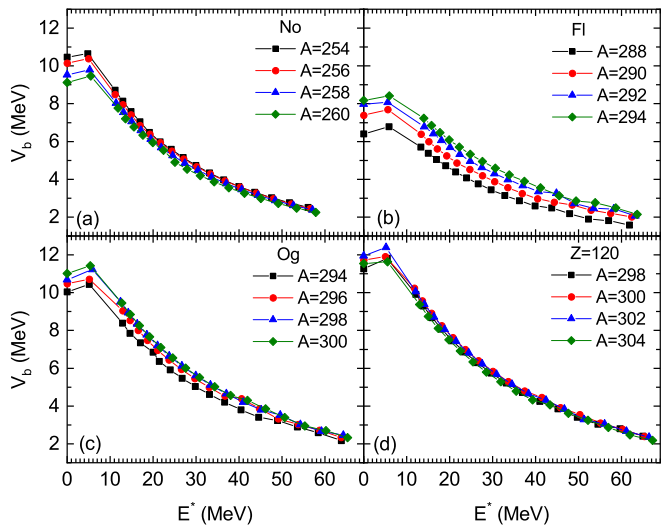

FIG. 3. Calculated fission barrier heights of No (a), Fl (b), Og (c), $Z = 120$ (d) isotopes are shown as a function of excitation energies.

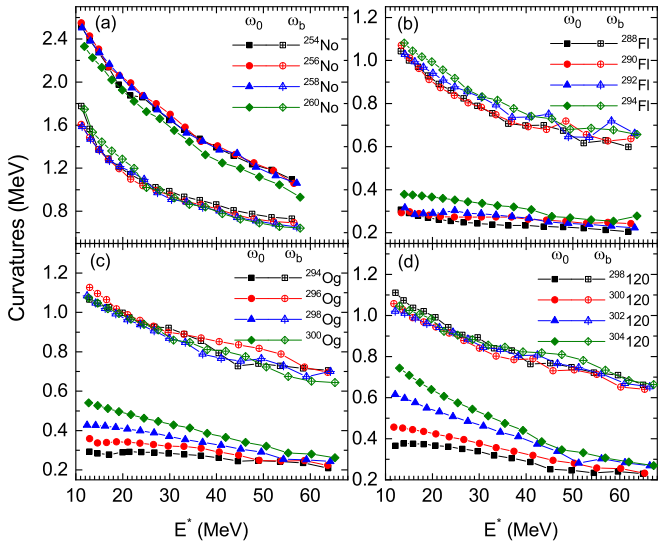

FIG. 4. Calculated curvatures around the equilibrium point (ω_0) and the barrier saddle point (ω_b) as a function of excitation energy, for No (a), Fl (b), Og (c), and $Z = 120$ (d) isotopes.

of fission barriers of superheavy nuclei can be very different from empirical models.

In addition to fission barrier heights, the curvatures of fission barriers also play an important role in calculations of fission rates. Figure 4 displays the calculated energy dependent curvatures ω_0 and ω_b, corresponding to the equilibrium point and the saddle point, respectively. Generally, ω_0 and ω_b decrease with increasing excitation energies, which leads to reduced fission rates. For No isotopes, ω_0 is larger than ω_b. For Fl, Og, and $Z = 120$ isotopes, ω_0 is very small, which means the fission valley is flat. Actually the ground state deformations of these nuclei are slightly oblate. The very small ω_0 can greatly enhance the stabilities of these nuclei against fission at high excitations.

Finally the first-chance survival probabilities $\Gamma_n/\Gamma_{\rm tot}$ of superheavy compound nuclei are calculated, as shown in Fig. 5. Different modelings for the survival probabilities: $R_1 = \frac{\Gamma_n^{\rm gas}}{\Gamma_n^{\rm gas}+\Gamma_{f2}}$, $R_2 = \frac{\Gamma_n^{BW}}{\Gamma_n^{BW}+\Gamma_{f2}}$, $R_3 = \frac{\Gamma_n^{\rm gas}}{\Gamma_n^{\rm gas}+\Gamma_{f1}}$, $R_4 = \frac{\Gamma_n^{BW}}{\Gamma_n^{BW}+\Gamma_{f1}}$, and $R_5 = \frac{\Gamma_n^{BW}}{\Gamma_n^{BW}+\Gamma_f^{BW}}$, are adopted for comparison. These modelings all are good for descriptions of fission probabilities of ^{210}Po.

In Fig. 5(a)–5(d), $\Gamma_n/\Gamma_{\rm tot}$ results for ^{254,256,258,260}No are shown. For ^{254}No, results from different approaches are close. The discrepancies between different modelings increase with increasing neutron numbers. We see that R_1 and R_3 are close, and R_2 and R_4 are close. This means that for No isotopes, the role of ω_0/T is not significant. At high excitations, R_1 (and R_2) is slightly larger than R_3 (and R_4) due to reduced ω_0/T, while it is on the contrary at low excitations. With the same fission widths, the survival probabilities with $\Gamma_n^{\rm gas}$ are obviously smaller than those with the statistical model at high excitations. At low excitations, the survival probabilities with $\Gamma_n^{\rm gas}$ are larger.

Figure 5(e)–5(h) displays the survival probabilities of ^{288,290,292,294}Fl isotopes. For ^{288}Fl, the fission barriers are lower than others, as shown in Fig. 3. Its survival probabilities are much smaller than 1.0 at low excitations, and then discrepancies are large. For ^{292,294}Fl with higher fission barriers, the first-chance survival probabilities all are close to 1.0 at low excitations. In experiments, the compound nuclei ^{290,292}Fl are produced in the hot fusion of ^{48}Ca + ^{242,244}Pu [10]. Generally the survival probabilities increase with increasing neutron numbers for Fl isotopes. Different from No isotopes, we see that with the same neutron evaporation width, the survival probabilities with Γ_{f2} are considerably larger than those with Γ_{f1}. This is because ω_0/T is very small for Fl isotopes at high excitations, which can significantly reduce fission widths. With the same fission widths, the survival probabilities with Γ_n^{BW} are much larger than those with $\Gamma_n^{\rm gas}$ at high excitations. For Fl isotopes, R_4 and R_5 are in the middle between different modelings, while they are among the largest for No isotopes.

The survival probabilities of ^{294,296,298,300}Og isotopes are shown in Fig. 5(i)–5(l). For $Z = 120$ isotopes, the results are shown in Fig. 5(m)–5(p). Note that the compound nucleus ^{297}Og is produced in the hot fusion of ^{48}Ca + ^{249}Cf [14]. The compound nuclei in synthesizing element 120 are ^{299,302}120 in attempted experiments [15,17–19]. The patterns of calculated survival probabilities of $Z = 120$ isotopes are very similar to those of ^{292,294}Fl and Og isotopes. The combination of Γ_n^{BW} and Γ_{f2} leads to the largest survival probabilities. Indeed, the factors ω_0/T are very small for Fl, Og, and $Z = 120$ isotopes at high excitations. The role of ω_0/T can be traced back to the dynamical Kramers model and is usually ignored in the Bohr-Wheeler model. In all cases, R_4 is close to R_5, which verified the correctness of the new formula. Note that the Bohr-Wheeler model results in very large fission widths about 1–2 MeV at high excitations in the superheavy region. Actually nuclear fission becomes very dissipative at high excitations [51]. If the fission width is about 1–2 MeV by the statistical model, then the later part of the fission from the saddle to the scission is not negligible at high excitations in real-time fission dynamics [56]. The statistical model also results in much larger neutron emission widths than the neutron gas model. We speculate that the same level density model used in both fission and neutron evaporation widths can have some offset effects.

Current calculations still invoke the phenomenological level densities, while employ the microscopic energy dependent fission barriers. The level density is essential for the microcanonical ensemble. Our results demonstrated that it is necessary to take into account the different level density parameters between the equilibrium point and the saddle point. Previously the deformation and energy dependent level density parameters could be obtained by calculating $S/2T$, or E/T^2, or $S^2/4E$ [29]. However, with these level densities, the fission probabilities of ^{210}Po cannot be well reproduced. With the current level densities and statistical models, the fission widths of superheavy nuclei would be as large as 1–2 MeV at high excitations, which is questionable. The reliable calculation of energy and deformation dependent level densities is another challenge [57]. Among different modelings, the neutron gas model always results in the lower limits of survival probabilities, which is also shown in ^{210}Po. In addition, the role of microscopically calculated curvatures is important

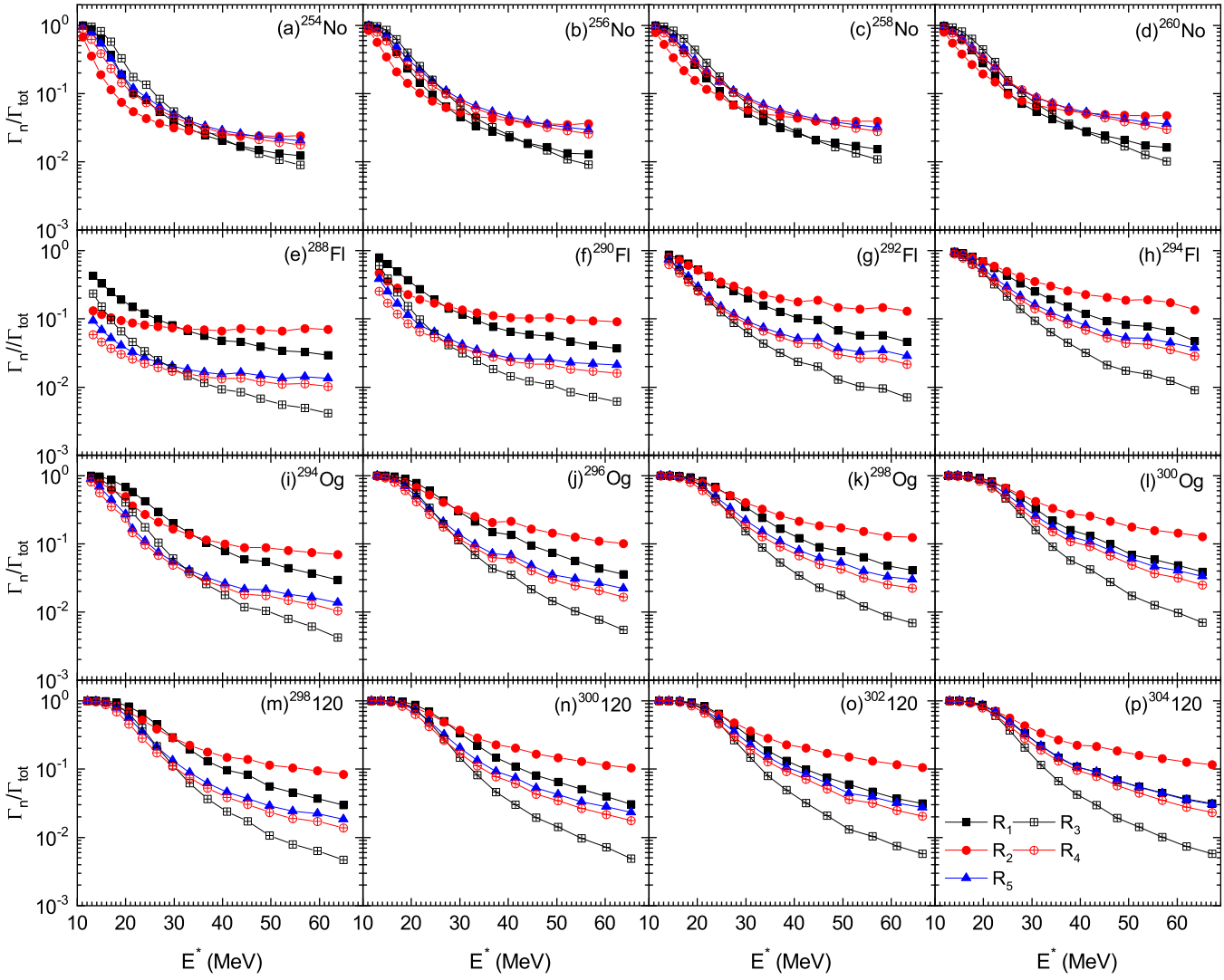

FIG. 5. Calculated first-chance survival probabilities $\Gamma_n/\Gamma_{\rm tot}$ of No, Fl, Og, and $Z = 120$ isotopes with various modelings. Results of ^{254,256,258,260}No are shown from (a) to (d); ^{288,290,292,294}Fl are shown from (e) to (d); ^{294,296,298,300}Og are shown from (i) to (l); ^{298,300,302,304}120 are shown from (m) to (p). Different modelings: $R_1 = \frac{\Gamma_n^{\rm gas}}{\Gamma_n^{\rm gas}+\Gamma_{f2}}$, $R_2 = \frac{\Gamma_n^{BW}}{\Gamma_n^{BW}+\Gamma_{f2}}$, $R_3 = \frac{\Gamma_n^{\rm gas}}{\Gamma_n^{\rm gas}+\Gamma_{f1}}$, $R_4 = \frac{\Gamma_n^{BW}}{\Gamma_n^{BW}+\Gamma_{f1}}$, and $R_5 = \frac{\Gamma_n^{BW}}{\Gamma_n^{BW}+\Gamma_f^{BW}}$, are shown for comparison.

in the superheavy region. Therefore, the optimistic modeling given by $R_2 = \Gamma_n^{BW}/(\Gamma_{f2} + \Gamma_n^{BW})$ should be more suitable, although the discrepancies between different modelings are large. Based on R_2 estimations, Fl and Og compound nuclei still have considerable survival probabilities at high excitations, which are crucial for the success of hot fusion reactions.

Since Fl, Og, and $Z = 120$ nuclei have similar considerable survival probabilities, the nonobservation of $Z = 119$ and 120 elements could be due to the reduced fusion probabilities of compound nuclei. In fact, the fusion probability using the ^{50}Ti projectile could be reduced by a factor of 5 compared to ^{48}Ca [18]. For element 119, the compound nucleus is ^{299}119 with an even number of neutrons [18], which is less favorable for the first-chance stability compared to the compound nucleus ^{297}Og with odd neutrons [14]. For the element 120, the cross section sensitivity has reached 200 fb [18], which is still not enough, considering the residue cross section of ^{294}Og is 0.3–0.5 pb [14]. For realistic calculations to guide experiments, the survival probabilities after multiple neutron emissions and the fusion reaction mechanism have to be studied in the future.

IV. SUMMARY

In summary, we studied the first-chance survival probabilities of heavy and superheavy nuclei at high excitations with microscopic temperature dependent fission barriers. There have been several experimental attempts to synthesize new superheavy elements $Z = 119$ and 120. Thus it is of interest to investigate various theoretical modelings of fission rates and survival probabilities. With a simple derivation, we demonstrated the relation between the Bohr-Wheeler model and the imaginary free energy method. The combination of the Bohr-Wheeler model and imaginary free energy method results in

a new formula for fission rates. To verify different modelings, the fission probabilities of ^{210}Po have been reproduced, demonstrating the essential role of energy dependent fission barriers. Next we studied the survival probabilities of No, Fl, Og, and $Z = 120$ isotopes with these modelings, which have large discrepancies in the superheavy region. We see that the curvatures ω_0 of the fission valley are very small for selected Fl, Og, and $Z = 120$ nuclei, which can greatly enhance their survival probabilities, although the role of curvatures is not significant in ^{210}Po. Besides, the microscopic neutron gas model results in smaller neutron emission widths and reduced survival probabilities. Therefore, the suitable modeling for survival probabilities is given by $\Gamma_n^{BW}/(\Gamma_{f2} + \Gamma_n^{BW})$. Actually, $Z = 120$ compound nuclei still have considerable first-chance survival probabilities at high excitations, which are very similar to those of Fl and Og nuclei. The nonobservation of $Z = 119$ and 120 elements could be due to the reduced fusion probabilities of compound nuclei. In the future, for more realistic modelings, survival probabilities after multiple neutron emissions will be studied.

ACKNOWLEDGMENTS

We thank the useful discussions with G. Adamian, A. Nasirov, and F. R. Xu. This work was supported by National Key R&D Program of China (Contract No. 2018YFA0404403), and the National Natural Science Foundation of China under Grants No. 11975032, 11790325, 11835001, and 11961141003.

[1] H. Haba, Nat. Chem. **11**, 10 (2019).
[2] S. A. Giuliani, Z. Matheson, W. Nazarewicz, E. Olsen, P.-G. Reinhard, J. Sadhukhan, B. Schuetrumpf, N. Schunck, and P. Schwerdtfeger, Rev. Mod. Phys. **91**, 011001 (2019).
[3] G. Münzenberg, S. Hofmann, F. P. Hesberger, W. Reisdorf, K. H. Schmidt, J. H. R. Schneider, P. Armbruster, C. C. Sahm, and B. Thuma, Z. Phys. A **300**, 107 (1981).
[4] G. Münzenberg, P. Armbruster, H. Folger, F. P. Hesberger, S. Hofmann, J. Keller, K. Poppensieker *et al.*, Z. Phys. A **317**, 235 (1984).
[5] G. Münzenberg, P. Armbruster, F. P. Hesberger, S. Hofmann, K. Poppensieker, W. Residorf, J. H. R. Schneider, W. F. W. Schneider, K.-H. Schmidt, C.-C. Sahm, and D. Vermeulen, Z. Phys. A **309**, 89 (1982).
[6] S. Hofmann, V. Ninov, F. P. Hesberger, P. Armbruster, H. Folger, G. Munzenberg *et al.*, Z. Phys. A **350**, 277 (1995).
[7] S. Hofmann, V. Ninov, F. P. Hesberger, P. Armbruster, H. Folger, G. Munzenberg *et al.*, Z. Phys. A **350**, 281 (1995).
[8] S. Hofmann, V. Ninov, F. P. Hesberger, P. Armbruster, H. Folger, G. Munzenberg *et al.*, Z. Phys. A **354**, 229 (1996).
[9] K. Morita, K. Morimoto, D. Kaji, T. Akiyama, S. Goto, H. Haba *et al.*, J. Phys. Soc. Jpn. **73**, 2593 (2004).
[10] Y. T. Oganessian, A. V. Yeremin, A. G. Popeko, S. L. Bogomolov, G. V. Buklanov, and M. L. Chelnokov *et al.*, Nature **400**, 242 (1999).
[11] Y. T. Oganessian, V. K. Utyonkov, Y. V. Lobanov, F. S. Abdullin, A. N. Polyakov, I. V. Shirokovsky, Y. S. Tsyganov, G. G. Gulbekian, S. L. Bogomolov, A. N. Mezentsev, S. Iliev, V. G. Subbotin, A. M. Sukhov, A. A. Voinov, G. V. Buklanov, K. Subotic, V. I. Zagrebaev, M. G. Itkis, J. B. Patin, K. J. Moody, J. F. Wild, M. A. Stoyer, N. J. Stoyer, D. A. Shaughnessy, J. M. Kenneally, and R. W. Lougheed, Phys. Rev. C **69**, 021601(R) (2004).
[12] Y. T. Oganessian, V. K. Utyonkov, Y. V. Lobanov, F. S. Abdullin, A. N. Polyakov, I. V. Shirokovsky, Y. S. Tsyganov, G. G. Gulbekian, S. L. Bogomolov, B. N. Gikal, A. N. Mezentsev, S. Iliev, V. G. Subbotin, A. M. Sukhov, O. V. Ivanov, G. V. Buklanov, K. Subotic, M. G. Itkis, K. J. Moody, J. F. Wild, N. J. Stoyer, M. A. Stoyer, R. W. Lougheed, C. A. Laue, Y. A. Karelin, and A. N. Tatarinov, Phys. Rev. C **63**, 011301(R) (2000).
[13] Y. T. Oganessian, F. S. Abdullin, P. D. Bailey, D. E. Benker, M. E. Bennett, S. N. Dmitriev, J. G. Ezold, J. H. Hamilton, R. A. Henderson, M. G. Itkis, Y. V. Lobanov, A. N. Mezentsev, K. J. Moody, S. L. Nelson, A. N. Polyakov, C. E. Porter, A. V. Ramayya, F. D. Riley, J. B. Roberto, M. A. Ryabinin, K. P. Rykaczewski, R. N. Sagaidak, D. A. Shaughnessy, I. V. Shirokovsky, M. A. Stoyer, V. G. Subbotin, R. Sudowe, A. M. Sukhov, Y. S. Tsyganov, V. K. Utyonkov, A. A. Voinov, G. K. Vostokin, and P. A. Wilk, Phys. Rev. Lett. **104**, 142502 (2010).
[14] Y. T. Oganessian, V. K. Utyonkov, Y. V. Lobanov, F. S. Abdullin, A. N. Polyakov, R. N. Sagaidak, I. V. Shirokovsky, Y. S. Tsyganov, A. A. Voinov, G. G. Gulbekian, S. L. Bogomolov, B. N. Gikal, A. N. Mezentsev, S. Iliev, V. G. Subbotin, A. M. Sukhov, K. Subotic, V. I. Zagrebaev, G. K. Vostokin, M. G. Itkis, K. J. Moody, J. B. Patin, D. A. Shaughnessy, M. A. Stoyer, N. J. Stoyer, P. A. Wilk, J. M. Kenneally, J. H. Landrum, J. F. Wild, and R. W. Lougheed, Phys. Rev. C **74**, 044602 (2006); Y. T. Oganessian, F. S. Abdullin, C. Alexander, J. Binder, R. A. Boll, S. N. Dmitriev, J. Ezold, K. Felker, J. M. Gostic, R. K. Grzywacz, J. H. Hamilton, R. A. Henderson, M. G. Itkis, K. Miernik, D. Miller, K. J. Moody, A. N. Polyakov, A. V. Ramayya, J. B. Roberto, M. A. Ryabinin, K. P. Rykaczewski, R. N. Sagaidak, D. A. Shaughnessy, I. V. Shirokovsky, M. V. Shumeiko, M. A. Stoyer, N. J. Stoyer, V. G. Subbotin, A. M. Sukhov, Y. S. Tsyganov, V. K. Utyonkov, A. A. Voinov, and G. K. Vostokin, Phys. Rev. Lett. **109**, 162501 (2012).
[15] Y. T. Oganessian, V. K. Utyonkov, Y. V. Lobanov, F. S. Abdullin, A. N. Polyakov, R. N. Sagaidak, I. V. Shirokovsky, Y. S. Tsyganov, A. A. Voinov, A. N. Mezentsev, V. G. Subbotin, A. M. Sukhov, K. Subotic, V. I. Zagrebaev, S. N. Dmitriev, R. A. Henderson, K. J. Moody, J. M. Kenneally, J. H. Landrum, D. A. Shaughnessy, M. A. Stoyer, N. J. Stoyer, and P. A. Wilk, Phys. Rev. C **79**, 024603 (2009).
[16] K. Chapman, Hunt for Element 119 to Begin, Chemistry World (September 12, 2017), https://www.chemistryworld.com/news/hunt-for-element-119-to-begin/3007977.article.
[17] S. Hofmann, J. Phys. G **42**, 114001 (2015).
[18] J. Khuyagbaatar, A. Yakushev, C. E. Dullmann, Ch. E. Dullmann, D. Ackermann, L.-L. Andersson *et al.*, Phys. Rev. C **102**, 064602 (2020).

[19] S. Hofmann, A. Heinz, R. Mann, J. Maurer, G. Munzenberg, S. Antalic *et al.*, Eur. Phys. J. A **52**, 180 (2016).
[20] M. G. Itkis, E. Vardaci, I. M. Itkis, G. N. Knyazheva, and E. M. Kozulin, Nucl. Phys. A **944**, 204 (2015).
[21] V. Zagrebaev and W. Greiner, Phys. Rev. C **78**, 034610 (2008).
[22] V. I. Zagrebaev, A. V. Karpov, and W. Greiner, Phys. Rev. C **85**, 014608 (2012).
[23] K. Siwek-Wilczynska, T. Cap, M. Kowal, A. Sobiczewski, and J. Wilczynski, Phys. Rev. C **86**, 014611 (2012).
[24] L. Liu, C. W. Shen, Q. F. Li, Y. Tu, X. B. Wang, and Y. J. Wang, Eur. Phys. J. A **52**, 35 (2016).
[25] F. Li, L. Zhu, Z. H. Wu, X. B. Yu, J. Su, and C. C. Guo, Phys. Rev. C **98**, 014618 (2018).
[26] L. Zhu, W. J. Xie, and F. S. Zhang, Phys. Rev. C **89**, 024615 (2014).
[27] J. H. Hamilton, S. Hofmann, and Y. T. Oganessian, Annu. Rev. Nucl. Part. Sci. **63**, 383 (2013).
[28] J. C. Pei, W. Nazarewicz, J. A. Sheikh, and A. K. Kerman, Phys. Rev. Lett. **102**, 192501 (2009).
[29] Y. Zhu and J. C. Pei, Phys. Scr. **92**, 114001 (2017).
[30] A. S. Zubov, G. G. Adamian, N. V. Antonenko, S. P. Ivanova, and W. Scheid, Phys. Rev. C **65**, 024308 (2002).
[31] C. J. Xia, B. X. Sun, E. G. Zhao, and S. G. Zhou, Sci. China Phys. Mech. Astron. **54**, 109 (2011).
[32] A. S. Zubov, G. G. Adamian, N. V. Antonenko, S. P. Ivanova, and W. Scheid, Eur. Phys. J. A **23**, 249 (2005).
[33] V. Weisskopf, Phys. Rev. **52**, 295 (1937).
[34] N. Bohr and J. A. Wheeler, Phys. Rev. **56**, 426 (1939).
[35] O. I. Davydovska, V. Yu. Denisov, and I. Yu. Sedykh, Phys. Rev. C **105**, 014620 (2022).
[36] M. G. Itkis, Y. T. Oganessian, and V. I. Zagrebaev, Phys. Rev. C **65**, 044602 (2002).
[37] J. Zhao, T. Niksic, D. Vretenar, and S. G. Zhou, Phys. Rev. C **99**, 014618 (2019).
[38] H. A. Kramers, Physica **7**, 284 (1940).
[39] I. Affleck, Phys. Rev. Lett. **46**, 388 (1981).
[40] Y. Zhu and J. C. Pei, Phys. Rev. C **94**, 024329 (2016).
[41] V. M. Strutinsky, Phys. Lett. B **47**, 121 (1973).
[42] K. H. Schmidt, Int. J. Mod. Phys. E **18**, 850 (2009).
[43] A. L. Goodman, Nucl. Phys. A **352**, 30 (1981).
[44] Y. Zhu and J. C. Pei, Phys. Rev. C **90**, 054316 (2014).
[45] J. C. Pei, W. Nazarewicz, J. A. Sheikh, and A. K. Kerman, Nucl. Phys. A **834**, 381c (2010).
[46] P.-G. Reinhard, B. Schuetrumpf, and J. Maruhn, Comput. Phys. Commun. **258**, 107603 (2021).
[47] J. Bartel, P. Quentin, M. Brack, C. Guet, and H. B. Hakansson, Nucl. Phys. A **386**, 79 (1982).
[48] J. Dobaczewski, W. Nazarewicz, and M. V. Stoitsov, Eur. Phys. J. A **15**, 21 (2002).
[49] A. Baran and Z. Lojewski, Acta Phys. Pol. B **25**, 1231 (1994).
[50] Y. Tanimura, D. Lacroix, and G. Scamps, Phys. Rev. C **92**, 034601 (2015).
[51] Y. Qiang and J. C. Pei, Phys. Rev. C **104**, 054604 (2021).
[52] P. Bonche, S. Levit, and D. Vautherin, Nucl. Phys. A **427**, 278 (1984).
[53] J. L. Egido and P. Ring, J. Phys. G **19**, 1 (1993)
[54] A. V. Ignatyuk, G. N. Smirenkin, M. G. Itkis, S. I. Mulgin, and V. N. Okolovich, Sov. J. Part. Nucl. **16**, 307 (1985).
[55] V. Yu. Denisov and I. Yu. Sedykh, Phys. Rev. C **98**, 024601 (2018).
[56] Y. Qiang, J. C. Pei, and P. D. Stevenson, Phys. Rev. C **103**, L031304 (2021).
[57] M. Bender, R. Bernard, G. Bertsch, S. Chiba, J. Dobaczewski, N. Dubray *et al.*, J. Phys. G **47**, 113002 (2020).